

Dynamic Target Interception in Cluttered Environments

Kevin Eckenhoff*, Indrajeet Yadav*, Guoquan Huang, and Herbert G. Tanner

Abstract—This abstract summarizes work on tightly coupling advanced estimation, navigation, and control algorithms to enable a unmanned aerial vehicle (UAV) to intercept and track a mobile ground target within an environment populated by obstacles. The UAV has to rely on its own perception system to localize itself, as well as detect and track its target, and utilize nonlinear motion planning and control algorithms to maneuver aggressively in order to intercept it. Although the static environment itself (obstacles) may be known to the UAV, the position and velocity of the target is not, giving rise to a problem that incorporates uncertainty and is of time-varying nature. The mathematical framework within which estimation and control are co-designed allows for provable formal guarantees of performance. The efficacy of the proposed approach is demonstrated through realistic simulations in Gazebo.

I. INTRODUCTION

The proposed approach *tightly* couples 3D visual-inertial navigation and target tracking, to provably establish (i) consistent and accurate robot and target localization, and (ii) convergence of the distance between robot and target to a pre-specified minimum safe distance. Estimating the relative position between detector and target is achieved with exclusive use of an inertial measurement unit (IMU) and a (stereo) camera, on the hardware side, and a lightweight multi-state constraint Kalman filter (MSCKF) [1] on the algorithmic side. Features are linearly marginalized to utilize their motion information without the need to store them in the state vector. The marginalization allows for the creation of constraints between the window poses while bounding the problem size, resulting in a computationally efficient estimation algorithm. This approach has been extended to include camera-to-IMU spatial and temporal calibration [2], to handle degenerate motions [3], and to enforce observability properties [4].

Aerial target tracking and navigation in a cluttered environment based on on-board estimation has been recently demonstrated in a case of tracking a spherical rolling target [5]. The latter approach employed a geometric approach similar to visual servoing, a receding horizon strategy that penalizes velocity and position errors, and a UAV motion control scheme based on minimum-snap trajectory generation [6]. So far, however, *provable* collision avoidance and target convergence guarantees are elusive, especially when considering nontrivial sensor platform dynamics. The approach described in this abstract achieves this by combining a new type of navigation functions developed for moving targets [7], with a geometric position and attitude tracking

UAV controller. The navigation function creates an almost globally attractive (to the target) vector field, which is utilized as a velocity reference for the UAV’s controller. Vector field tracking has been entertained in earlier work [8], but neither for the purpose of intercepting moving targets, nor in non-spherical workspace topologies and without full knowledge of robot and target states [9]. This work contributes in (i) extending visual-inertial navigation systems (VINS) to tightly-coupled 3D visual-inertial localization and target tracking, and (ii) integrating geometric UAV control with time-varying navigation functions in star-forests of obstacles. The approach is validated in ROS/Gazebo simulations.

A. UAV Control

Let m denote the mass of the quadrotor UAV, $\mathbf{J} \in \mathbb{R}^{3 \times 3}$ its moment of inertia about a frame aligned with the principal axes and attached at the center of mass cg , and ${}^M\mathbf{g}$ the acceleration of gravity in the inertial frame. The relative orientation between the inertial frame and the principal one at the UAV’s center of mass is captured by the rotation matrix ${}^M\mathbf{R} \in \text{SO}(3)$. The quantities ${}^M\mathbf{p}(t)$ and ${}^M\mathbf{p}_T(t) \in \mathbb{R}^3$ denote the position of the UAV and the target, respectively, in the inertial (MAP) frame. Take r to be the radius of the spherical bubble around the target and define the goal for navigation as minimizing the function $J({}^M\mathbf{p}, {}^M\mathbf{p}_T) = \|\mathbf{p} - \mathbf{p}_T\|^2 - r^2$. Let $\{0, \dots, S\}$ be an index set of *spherical* obstacles, including the workspace’s outer boundary indexed 0, and for $i \in \{0, \dots, S\}$, denote ρ_i, o_i , the center and radius of each obstacle, respectively. Define $\beta_0({}^M\mathbf{p}, {}^M\mathbf{p}_T) = \rho_0^2 - \|\mathbf{p} - o_0\|^2$ to be the workspace boundary, and $\beta_i({}^M\mathbf{p}, {}^M\mathbf{p}_T) = \|\mathbf{p} - o_i\|^2 - \rho_i^2$ any other interior obstacle. Let $\beta({}^M\mathbf{p}, {}^M\mathbf{p}_T) = \prod_{i=0}^S \beta_i({}^M\mathbf{p}, {}^M\mathbf{p}_T)$. It can be shown [7] that there exists a positive number N such that $\forall k \geq N$, and for a suitably large parameter $\lambda \in \mathbb{R}_+$, $({}^M\mathbf{p}, {}^M\mathbf{p}_T) = \frac{J({}^M\mathbf{p}, {}^M\mathbf{p}_T)}{[J({}^M\mathbf{p}, {}^M\mathbf{p}_T)^k + \lambda \beta({}^M\mathbf{p}, {}^M\mathbf{p}_T)]^{1/k}}$ has navigation function properties on a sphere world \mathcal{S} with a suitably chosen λ . For a diffeomorphism $h_{\lambda_{\text{sq}}}$ parameterized by a suitably chosen parameter $\lambda_{\text{sq}} \in \mathbb{R}_+$, mapping a *star world* \mathcal{F} to a *forest of stars* in the form of three-dimensional *squirrels* [10], the composition $\varphi = \tilde{\varphi} \circ h_{\lambda_{\text{sq}}}$ can also be shown [10] to have navigation function properties on \mathcal{F} .

Let the linear and angular velocity of the UAV relative to the inertial frame be denoted ${}^M\mathbf{v}$ and ${}^M\boldsymbol{\omega}$, respectively, and the angular velocity vector relative to the body cg frame be ${}^{\text{cg}}\boldsymbol{\omega}$. If v_{max} is the vehicle’s maximum speed, and k is a positive control gain, then a velocity reference relative to the inertial frame can be defined as ${}^M\mathbf{v}_d \triangleq -\text{erf}(k(\|\mathbf{p} - \mathbf{p}_T\| - r)) \cdot \frac{\nabla_{\mathbf{p}}\varphi}{\|\nabla_{\mathbf{p}}\varphi\|} \cdot v_{\text{max}}$. The velocity error for the UAV would then be $\mathbf{e}_v \triangleq {}^M\mathbf{v} - {}^M\mathbf{v}_d$. Let

*These authors contributed equally to this work.

This work leverages results from ARL MAST CTA #W911NF-08-2-0004, and is partially supported by DTRA (HDTRA1-16-1-0039).

The authors are with the Department of Mechanical Engineering, University of Delaware, Newark, DE 19716. Email: {keck, indragt, ghuang, btanner}@udel.edu

$\hat{\cdot} : \mathbb{R}^3 \rightarrow \mathfrak{so}(3)$ denote the wedge operation. With ${}^M_{cg}\mathbf{R}_d$ and ω_d denoting some desired UAV orientation and angular velocity for the UAV, respectively, the orientation and angular velocity errors are $\hat{\mathbf{e}}_R = \frac{1}{2}({}^M_{cg}\mathbf{R}_d^T {}^M_{cg}\mathbf{R} - {}^M_{cg}\mathbf{R}_d^T {}^M_{cg}\mathbf{R})$, $\mathbf{e}_\omega = {}^{cg}\boldsymbol{\omega} - {}^M_{cg}\mathbf{R}_d^T {}^M_{cg}\mathbf{R} {}^{cg}\boldsymbol{\omega}_d$; with k_v , k_R and k_ω being positive control gains for velocity, orientation, and angular velocity, the control inputs for the UAV (total thrust f and total moment \mathbf{M} relative to cg) can be set as (cf. [11])

$$f = (-k_v \mathbf{e}_v + m {}^M\mathbf{g} + m {}^M\dot{\mathbf{v}}_d) \cdot ({}^M_{cg}\mathbf{R} \frac{{}^M\mathbf{g}}{\|{}^M\mathbf{g}\|})$$

$$\mathbf{M} = -k_R \mathbf{e}_R - k_\omega \mathbf{e}_\omega + {}^{cg}\boldsymbol{\omega} \times \mathbf{J} {}^{cg}\boldsymbol{\omega}$$

making \mathbf{e}_v , \mathbf{e}_R , and \mathbf{e}_ω converge exponentially to zero.

II. STATE ESTIMATION

It is assumed that the UAV is only equipped with an IMU, providing linear acceleration and angular velocity readings, and a set of stereo cameras. Taking into account the limited computational resources on the UAV, and the need for low-latency, a filtering-based VINS solution known as the MSCKF [1] is now extended and applied to this problem. With \mathcal{G} denoting the IMU's global frame and \mathcal{I}_k the IMU's local frame at step k , the state representation for the UAV's IMU at time step k can be written $\mathbf{x}_{\text{IMU},k} = [\mathcal{I}_k \bar{\mathbf{q}}^T \quad \mathbf{b}_{w_k}^T \quad \mathcal{G}\mathbf{v}_k^T \quad \mathbf{b}_{a_k}^T \quad \mathcal{G}\mathbf{p}_k^T]^T$, which includes the unit quaternion parameterizing the rotation from the global frame to the local IMU frame, gyro bias, global velocity, accelerometer bias, and global position, respectively. The state of the target, $\mathbf{T} \in \mathbb{R}^{3n+3}$, is parameterized using a constant derivative model of order n , in which $\mathcal{G}\mathbf{p}_{T_k}^{(i)}$ denotes the i th derivative of the target's position $\mathbf{T}_k = [\mathcal{G}\mathbf{p}_{T_k}^T \quad \mathcal{G}\mathbf{p}_{T_k}^{(1)T} \quad \mathcal{G}\mathbf{p}_{T_k}^{(2)T} \quad \dots \quad \mathcal{G}\mathbf{p}_{T_k}^{(n)T}]^T$. Letting now \mathbf{n}_T denote a Gaussian noise vector, the target is assumed to evolve as $\mathcal{G}\mathbf{p}_{T_k}^{(i)} = \mathcal{G}\mathbf{p}_{T_{k+1}}^{(i+1)}$, $\mathcal{G}\mathbf{p}_{T_k}^{(n)} = \mathbf{n}_T$ giving rise to a linear target evolution model—which allows for simple integration into the filter propagation step. Due to performing localization in a previous map, a 1-DOF relative quaternion (corresponding to yaw), ${}^M_{\mathcal{G}}\bar{\mathbf{q}}$ and relative position between the IMU's global frame and the prior map frame, $\mathcal{G}\mathbf{p}_M$ are also estimated. Bearing measurements to known landmarks and the target, as seen from pair of stereo cameras, are utilized in the standard EKF manner. Meanwhile, bearing measurements to *unknown* features are processed through the computationally efficient MSCKF update step.

III. SYSTEM VALIDATION

In the validation scenario, a UAV (Firefly) equipped with a 20° downward facing VI-sensor intercepts a target (realized by a turtlebot). The target moves in a straight line with a velocity of 1 m/s and the UAV intercepts it with a maximum speed of 6 m/s. The motion planning process consists of three phases: (i) hovering at 2 m using a position controller to initialize the tracking, (ii) target chase using the navigation function based planner and velocity controller, and (iii) hovering again using the position controller once the target crosses the detection area. Figures 1(a) and 1(b) show the x , y and z components of the error between estimates, and ground truth positions of the UAV and the target.

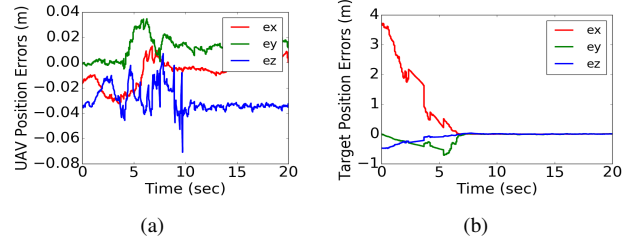


Fig. 1. (a) VINS UAV position estimate errors; (a) Target errors.

IV. CONCLUSION

For dynamic ground target interception and tracking by an UAV flying in constrained, unstructured (e.g., without motion capture) and GPS-denied environments, a tightly-coupled estimation and nonlinear control approach proves effective. The approach utilizes an extension of a visual-inertial navigation methodology based on MSCKF, and a navigation function-based geometric UAV tracking controller, that is informed about the vehicle's location, as well as that of the target, by the on-board estimator. The combined estimation-control architecture has been validated in Gazebo and current efforts are directed at outdoor field experiments.

REFERENCES

- [1] A. I. Mourikis and S. I. Roumeliotis, "A multi-state constraint Kalman filter for vision-aided inertial navigation," in *Proceedings of the IEEE International Conference on Robotics and Automation*, Rome, Italy, Apr. 10–14, 2007, pp. 3565–3572.
- [2] M. Li and A. I. Mourikis, "Online temporal calibration for Camera-IMU systems: Theory and algorithms," *International Journal of Robotics Research*, vol. 33, no. 7, pp. 947–964, Jun. 2014.
- [3] D. Kottas, K. Wu, and S. Roumeliotis, "Detecting and dealing with hovering maneuvers in vision-aided inertial navigation systems," in *Proceedings of the IEEE/RSJ International Conference on Intelligent Robots and Systems*, Nov. 2013, pp. 3172–3179.
- [4] J. Hesch, D. Kottas, S. Bowman, and S. Roumeliotis, "Consistency analysis and improvement of vision-aided inertial navigation," *IEEE Transactions on Robotics*, vol. PP, no. 99, pp. 1–19, 2013.
- [5] J. Thomas, J. Welde, G. Loianno, K. Daniilidis, and V. Kumar, "Autonomous flight for detection, localization, and tracking of moving targets with a small quadrotor," *IEEE Robotics and Automation Letters*, vol. 2, no. 3, pp. 1762–1769, July 2017.
- [6] D. Mellinger and V. Kumar, "Minimum snap trajectory generation and control for quadrotors," in *Proc. of the IEEE International Conference on Robotics and Automation*, Shanghai, China, May 9–13, 2011, pp. 2520–2525.
- [7] J. Sun and H. G. Tanner, "Constrained decision-making for low-count radiation detection by mobile sensors," *Autonomous Robots*, vol. 39, no. 4, pp. 519–536, 2015.
- [8] D. Zhou and M. Schwager, "Vector field following for quadrotors using differential flatness," in *Proceedings of the IEEE International Conference on Robotics and Automation*, May 2014, pp. 6567–6572.
- [9] G. P. Roussos, D. V. Dimarogonas, and K. J. Kyriakopoulos, "3d navigation and collision avoidance for a non-holonomic vehicle," in *Proceedings of the American Control Conference*, June 2008, pp. 3512–3517.
- [10] C. Li, "Star-world navigation functions for convergence to a time-varying destination manifold," Master's thesis, University of Delaware, 2017.
- [11] T. Lee, M. Leoky, and N. H. McClamroch, "Geometric tracking control of a quadrotor uav on SE(3)," in *Proceedings of the 49th IEEE Conference on Decision and Control*, Dec 2010, pp. 5420–5425.